



University of Warwick institutional repository: <http://go.warwick.ac.uk/wrap>

This paper is made available online in accordance with publisher policies. Please scroll down to view the document itself. Please refer to the repository record for this item and our policy information available from the repository home page for further information.

To see the final version of this paper please visit the publisher's website. Access to the published version may require a subscription.

Author(s): N. A. Khovanova and J. Windelen

Article Title: Minimal energy control of a nanoelectromechanical memory element

Year of publication: 2012

Link to published article:

<http://dx.doi.org/10.1063/1.4736566>

Publisher statement: Copyright 2012 American Institute of Physics.

This article may be downloaded for personal use only. Any other use requires prior permission of the author and the American Institute of Physics.

The following article appeared in Khovananova, N. A. and Windelen, J. (2012). Minimal energy control of a nanoelectromechanical memory element . Applied Physics Letters, 101(2), pp. 024104 (citation of published article) and may be found at [http://apl.aip.org/resource/1/applab/v101/i2/p024104\\_s1?isAuthorized=no](http://apl.aip.org/resource/1/applab/v101/i2/p024104_s1?isAuthorized=no)

# Minimal energy control of a nanoelectromechanical memory element

N. A. Khovanova<sup>a)</sup> and J. Windelen

*School of Engineering, University of Warwick, Coventry CV4 7AL, United Kingdom*

The Pontryagin minimal energy control approach has been applied to minimise the switching energy in a nanoelectromechanical memory system and to characterise global stability of the oscillatory states of the bistable memory element. A comparison of two previously experimentally determined pulse-type control signals with Pontryagin control function has been performed and the superiority of the Pontryagin approach with regard to power consumption has been demonstrated. An analysis of global stability shows how values of minimal energy can be utilized in order to specify equally stable states.

PACS numbers: 05.45.-a, 85.85.+j, 02.30.Yy

Keywords: NEMS, memory element, oscillatory state, optimal control

The feasibility of the use of a nanoelectromechanical system (NEMS) as a memory element has been demonstrated in a number of experimental investigations<sup>1-8</sup>. It has been suggested that in order to increase the frequency of operation, oscillatory states (cycles) should be used as the stationary states of memory elements, with consequential switching between two cycles. An oscillatory state is achieved by applying an external harmonic driving force and by selecting the driving amplitude and frequency in the range of hysteresis, observed for nonlinear resonance<sup>1,4-8</sup>. Such oscillatory states are principally different from the stationary states, i.e. fixed points - traditionally used in the majority of digital processing and storage devices<sup>2,3,9</sup>, and the analysis of the oscillatory states is much more challenging<sup>10,11</sup>.

Existing switching control strategies developed for the fixed points are also not directly applicable. The switching between the states is induced by an external control signal. Various strategies to control the switching have been discussed and experimentally validated<sup>1,4-8</sup>. A complex dependence of switching on parameters of the control signal was observed by Unterreithmeier et al<sup>4</sup>. Noh et al<sup>6</sup> discussed how to decrease the time of switching and concluded that a reduced quality factor significantly shortens the time. Another important parameter, the energy of the control force, has not been considered. This is also true for characterization of the stability of oscillatory states beyond local stability, which however can be explained by the absence of a corresponding generic approach.

By applying Pontryagin's theory of optimal control<sup>12,13</sup> we consider the *minimal* energy control of switching between oscillatory states of a nonlinear bistable NEMS followed by a discussion of the global stability of the states. The Pontryagin approach does not restrict the control force to a particular shape, and allows an analysis of global stability of the oscillatory states via estimation of the height of a quasi-potential, which is an analogue to the Lyapunov functional<sup>13,14</sup>. The link between global stability and optimal control is

based on an analogy between the Hamiltonian theory of fluctuations and Hamiltonian formulation of the control problem<sup>12,13</sup>. This has been used previously to achieve switching control in chaotic systems<sup>13,15</sup> via analysis of fluctuational trajectories. Recently, the reversibility between fluctuational activation paths and relaxation paths in the potential systems was used in a discussion of spin-torque switches in a ferromagnetic layer<sup>16</sup>. Note that since the memory element considered here is a non-potential system, the approach based on the reversibility between activation and relaxation paths is not applicable and therefore the more generic Pontryagin approach has been applied<sup>12,13</sup>.

We further consider two specific types of control signals, previously demonstrated experimentally<sup>4,7</sup>. These have limitations on their possible shapes and only three parameters can be included in the energy optimization task: amplitude, duration and phase related to the periodic driving signal. In the present study, we identified the optimal values of the parameters corresponding to *minimal* energies of the control signals, as this aspect has not been considered before, and compared the minimal energies with the solution of the Pontryagin minimal energy control task. Finally, the global stability of the cycles versus system parameters is analysed.

The dynamics of a memory element based on NEMS can be described by the nonlinear oscillator model<sup>4,7,10</sup>

$$\begin{aligned} \dot{x}_1 &= K_1(\mathbf{x}(t)) = x_2, \\ \dot{x}_2 &= K_2(\mathbf{x}(t)) = -\alpha x_2 - \omega_0^2 x_1 - a x_1^3 \\ &\quad + A \cos \Omega t + u(t) \end{aligned} \quad (1)$$

In (1)  $\mathbf{x}(t) = [x_1(t), x_2(t)]$  is the state space vector,  $x_1$  and  $x_2$  correspond to the displacement and velocity of the NEMS cantilever, respectively;  $\alpha$  is a damping coefficient,  $\omega_0^2$  and  $a$  characterize non-damped eigenfrequency and nonlinearity respectively,  $A$  and  $\Omega$  correspond to the amplitude and frequency of the harmonic driving signal and  $u(t)$  is a control function representing the force inducing switching.

We fixed the values of the parameters of the oscillator as  $\alpha = 0.01$ ,  $\omega_0 = 1$  and  $a = 1$ , and the amplitude of the harmonic driving force  $A = 0.075$ . Note that equation (1) is written in normalized dimensionless units; the value of

---

<sup>a)</sup>Electronic mail: n.khovanova@warwick.ac.uk

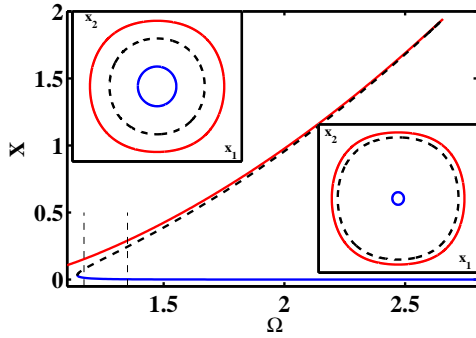


FIG. 1. Dependence of amplitude  $X$  of the cycles on driving frequency  $\Omega$ ;  $X = \frac{1}{2} \int_0^T x_1^2(t) dt$ ,  $T = 2\pi/\Omega$ . Solid (red and blue) lines correspond to the stable cycles  $C_l$  and  $C_s$ , respectively and dashed black line refers to saddle cycle  $C$ . Thin dashed vertical lines denote the values  $\Omega = 1.17$  and  $\Omega = 1.34$ . Insets: the cycles in the state space for  $\Omega = 1.17$  (upper left) and  $\Omega = 1.34$  (lower right).

$\alpha$  is chosen to represent a typical value of the quality factor observed in the experiments<sup>1,4-8</sup>. For the selected value of  $A$ , a hysteresis is observed in the frequency range  $\Omega \in (1.142 : 2.657)$  (Fig. 1). In this system, three cycles, two stable and one saddle, coexist in the hysteresis region, the boundary of which is defined by saddle-node bifurcations.

Our initial choice of the operational point of the memory element is located at frequency  $\Omega = 1.17$ . For this value of  $\Omega$ , the amplitude  $S$  of the saddle cycle lies approximately in the middle (left insert in Fig. 1) between the amplitudes of the two stable cycles  $C_s$  and  $C_l$  (indices  $s$  and  $l$  define small and large cycles). The rationale for such a choice of the operational point is an assumption that the stability of the cycles is reflected in the central location of the saddle cycle in the phase space, and hence in its amplitude. It is noteworthy that the multipliers of both stable cycles are equal within the whole hysteresis region (except in the extremely small region in the vicinity of the saddle-node bifurcation), thus indicating that the stable cycles have the same *local* stability. This is however not the case for *global* stability as discussed below.

Several different approaches to control switching were experimentally determined<sup>4-8</sup>. We consider two<sup>4,7</sup> which are compatible with the additive form of the control term in (1). Initially, the system resides in the oscillatory state  $C_l$  (or  $C_s$ ) and then switches to another state  $C_s$  (or  $C_l$ ).

The first type of function  $u_1(t)$  corresponds to a single pulse of amplitude  $u_0$  and duration  $\tau$  acting at time moment  $t_0$

$$u_1(t) = \begin{cases} \pm u_0 & \text{if } t_0 \leq t \leq t_0 + \tau \\ 0 & \text{otherwise} \end{cases} \quad (2)$$

This form of control assumes an instantaneous push of the system. The sign of  $u_0$  is positive if there is a transition from the cycle with a small amplitude to the cycle

with a large amplitude ( $C_s \rightarrow C_l$ ), and the sign is negative for the opposite transition ( $C_l \rightarrow C_s$ ).

The second type of the control function  $u_2(t)$  has the following form

$$u_2(t) = \begin{cases} \pm u_0 \cos \Omega t & \text{if } t_0 \leq t \leq t_0 + \tau \\ 0 & \text{otherwise} \end{cases} \quad (3)$$

In this way the control function  $u_2(t)$  increases amplitude of the harmonic driving force for a certain period of time  $\tau$ . Both functions  $u_1(t)$  and  $u_2(t)$  depend on three parameters: amplitude  $u_0$ , duration  $\tau$  and initial time  $t_0$ . The time  $t_0$  is related to the phase of the harmonic driving force as  $\phi_0 = \Omega t_0$ , and therefore we use phase  $\phi_0$  instead of  $t_0$ ; the phase lies in the finite interval  $\phi_0 \in (0 : 2\pi]$ .

The energy minimal control task consists in finding the control function  $u(t)$  with minimal energy  $J$

$$J = \int_{t_0}^{t_f} u^2(t) dt \quad (4)$$

where  $t_0$  and  $t_f$  define time interval with nonzero control function. For the functions specified by (2) and (3), the solution of this control problem leads to particular values of the amplitude  $u_0$ , duration  $\tau$  and phase  $\phi_0$  corresponding to minimal energies  $J_m$ .

If we allow an *arbitrary* shape of  $u(t)$  then the solution of the control task corresponds to the solution of a boundary value problem for the following Pontryagin Hamiltonian system<sup>12,13</sup>:

$$\dot{x}_i = \frac{\partial H}{\partial p_i}, \quad \dot{p}_i = -\frac{\partial H}{\partial x_i}, \quad i = \{1, 2\} \quad (5)$$

$$H = H(\mathbf{x}(t), \mathbf{p}(t)) = 1/2 p_2^2 + p_1 K_1 + p_2 K_2 \quad (6)$$

with the boundary conditions on the cycles  $C_l$  (or  $C_s$ ) and the saddle cycle  $S$  (see for further details<sup>17,18</sup>). Note that all cycles of (1) are present in (5) for  $\mathbf{p} = 0$ , but they become saddle<sup>13,18</sup>. So the solution of the boundary value problem specifies a heteroclinic trajectory  $(\mathbf{x}^h(t), \mathbf{p}^h(t))$  of (5)<sup>17,18</sup>. Variable  $p_2^h(t)$  yields the Pontryagin control function  $u(t)$  and consequently the minimal energy  $J_m^p$ . Integral  $J(t) = \int_{t_0}^t [p_2(t)]^2 dt$  is nondecreasing along any trajectory of (5) and it can be used as a generalized Lyapunov function for a deterministic system (1)<sup>13,14</sup>. It implies that the value of  $J_m^p$  corresponds to a potential barrier between oscillatory states and therefore specifies the global stability of the cycles in (1).

The energy  $J$  is dependent on the duration  $\tau$  and phase  $\phi_0$  of the control signals (2) and (3), as shown in Fig. 2. The value  $J$  was obtained by finding a minimal value of amplitude  $u_0$  inducing the transition between cycles for fixed values of  $\tau$  and  $\phi_0$ . The patterns of the graphs (Fig. 2) for two control signals  $u_1(t)$  and  $u_2(t)$  are distinct. The single pulse control  $u_1(t)$  is characterized by a strong dependence on the initial phase  $\phi_0$  (Fig. 2 (a)) and the energy varies by several orders of magnitude for different  $\phi_0$ . Thus, the initial phase  $\phi_0$  is an important parameter for function  $u_1(t)$ . Energy  $J$  is larger for the

pulse control  $u_1(t)$  than for  $u_2(t)$ . In both cases for  $u_1(t)$  and  $u_2(t)$ , the energy  $J$  is significantly larger for the transition  $C_l \rightarrow C_s$  than for the reverse transition, inferring that the larger cycle  $C_l$  is more stable to perturbations than the smaller one  $C_s$ .

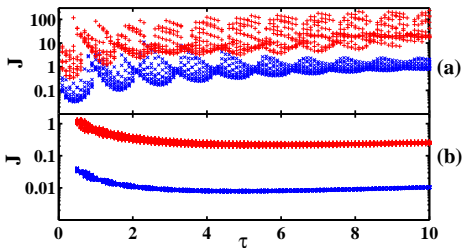


FIG. 2. Dependence of energy  $J$  on duration  $\tau$  for different phases  $\phi_0$ : (a) for control force  $u_1(t)$ , (b) for control force  $u_2(t)$ . Markers + (red, upper set of markers) and  $\times$  (blue, lower set of markers) correspond to transitions  $C_l \rightarrow C_s$  and  $C_s \rightarrow C_l$ , respectively.

The minimal energy  $J_m$  is observed for a particular set of parameters as shown in Table 1. The set depends on the type of the control function  $u_1(t)$  or  $u_2(t)$  as well as the direction of switching  $C_l \rightarrow C_s$  or  $C_s \rightarrow C_l$ . For example, the duration  $\tau$  of the control pulse  $u_1(t)$  corresponding to minimal energy is less than one period of harmonic driving signal, whereas  $\tau$  of  $u_2(t)$  is of the order of several periods. These durations define the so-called *activation* part of control which corresponds to the transition from the initial stable cycle to the saddle cycle (separatrix), forming the boundary between the basins of attraction of the stable cycles. After reaching the separatrix following the activation path, the system relaxes to another stable cycle along the *relaxation* path. This path is significantly longer and depends on the value of damping coefficient  $\alpha$ . The relaxation part mainly contributes to the duration of switches as previously discussed<sup>4</sup>.

We compared, in the next step, the minimal energies of  $u_1(t)$  and  $u_2(t)$  with the result of Pontryagin control corresponding to arbitrary  $u(t)$ . Since the solution of the Pontryagin control specifies a heteroclinic trajectory<sup>17,18</sup>, the duration of the control function should be infinite. However, the infinite duration results from an exponential decay of  $p_2^h(t)$  to the zero value in the vicinity of stable cycles. Applying a cut off point where the function has a small but non-zero value,  $p_2^h(t)$  can be made finite. This is achieved by shifting the initial and final times of  $p_2^h(t)$ , i.e. by truncating the low amplitude parts of  $p_2^h(t)$ . The resulting truncated control functions  $u_t(t)$  are shown in Fig. 3 (b) along with trajectories  $x_n \equiv x_1(nT)$  in stroboscopic section (Fig. 3 (a)). The trajectories  $x_n$  have been obtained by applying  $u_t(t)$  in (1). Thus, we have verified that the truncated functions  $u_t(t)$  induced the necessary transitions without changing the optimal energy  $J_m^p$  (Table 1).

The duration of the control functions (Fig. 3 (b)) is comparable with relaxation time during switching. Am-

	$u_1, C_s$	$u_2, C_s$	$u_t, C_s$	$u_1, C_l$	$u_2, C_l$	$u_t, C_l$
$J_m$	0.032	0.0075	0.00116	0.318	0.192	0.016
$J_m/J_m^p$	22	6.5	1	20	12	1
$u_0$	0.115	0.025		0.443	0.011	
$\tau$	0.450	4.500	141	0.300	5.500	142
$\phi_0$	0.685	0.260		0.100	0.010	
$P_m$	0.06	$9.4 \times 10^{-4}$	$8.3 \times 10^{-6}$	0.600	0.010	$1.1 \times 10^{-4}$
$P_m/P_m^p$	7237	113	1	5217	87	1
$u_0$	0.105	0.019		0.332	0.065	
$\tau$	1.700	24.10	141	6.000	60.90	142
$\phi_0$	0.560	0.235		0.010	0.010	

TABLE I. Optimal values of the amplitude  $u_0$ , duration  $\tau$  and phase  $\phi_0$  corresponding to the minimal energy  $J_m$  and minimal power  $P_m$  for different control functions. The first row specifies the type of control function and the initial state ( $u_t$  refers to arbitrary form as in (1)).  $J_m/J_m^p$  define the ratio of  $J_m$  to the minimal energy of Pontryagin control  $J_m^p$ , calculated for each initial state separately. Values of  $P_m$  correspond to the minimal power  $J_m/\tau$  and  $P_m^p$  to Pontryagin control. Ratio  $P_m/P_m^p$  was calculated separately for each initial oscillatory state.

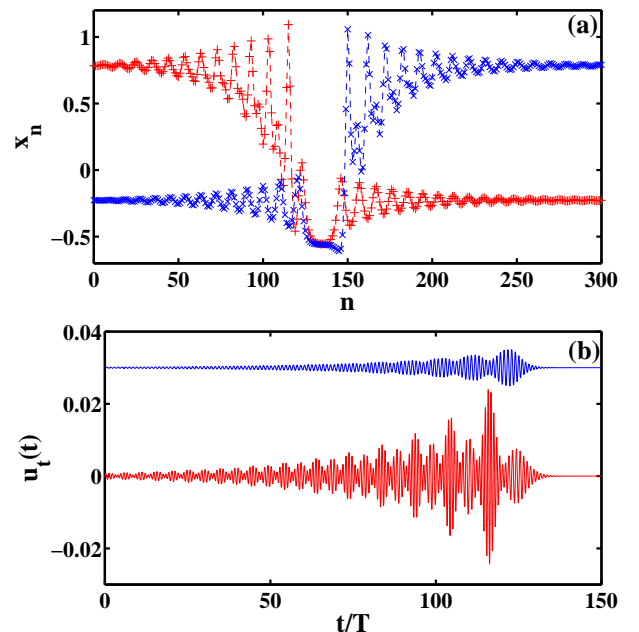


FIG. 3. (a) Trajectories during Pontryagin control and (b) respective control functions  $u_t(t)$ . (a) Points shown correspond to coordinates  $x_1(nT) \equiv x_n$  in the stroboscopic section taken after each period  $T = 2\pi/\Omega$  of the harmonic driving force. Markers + (red) and  $\times$  (blue) reflect the transitions  $C_l \rightarrow C_s$  and  $C_s \rightarrow C_l$ , respectively. (b) Lower red line represents the truncated control function  $u_t(t)$  for transition  $C_l \rightarrow C_s$  and upper blue line refers to  $C_s \rightarrow C_l$ . The upper function is shifted by +0.03 for an illustrative purpose.

plitude of  $u_t(t)$  is less than the amplitude  $A$  of the harmonic driving force and the energy  $J_m^p$  is smaller by an order of magnitude than energy  $J_m$  for control functions

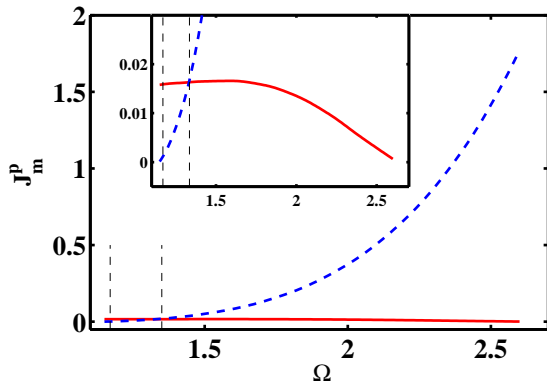


FIG. 4. Barrier  $J_m^p$  as a function of driving frequency  $\Omega$ . Solid (red) and dashed (blue) lines correspond to the stable cycles  $C_l$  and  $C_s$ , respectively. Thin dashed vertical lines denote values  $\Omega = 1.17$  and  $\Omega = 1.34$ . The inset shows a magnified part of the figure.

$u_1(t)$  and  $u_2(t)$  (Table 1). The difference between the pulse-type control functions ( $u_1(t), u_2(t)$ ) and the Pontryagin control function  $u_t$  becomes more pronounced, if instead of energy the power  $P_m$  of control is considered, i.e. ratio  $J/\tau$  (Table 1): for  $u_t$ , 4 orders of magnitude less power than for  $u_1(t)$  (or 2 orders of magnitude than for  $u_2(t)$ ) is required to perform a switch between two stable states.

The value of  $J_m^p$ , found for arbitrary  $u(t)$  via solving (4) and (5), provides a minimal value of control energy and can be used as a reference point for the design of a control function. Specific features of the shape of  $u_t(t)$  can be used for designing a sub-optimal force, as discussed previously<sup>17,19</sup>. It can be seen from Fig. 3 (b) that the shape of the control functions  $u_t(t)$  depends on the direction of switching. The Pontryagin approach along with two other control functions (2) and (3) shows that the cycle  $C_l$  is significantly more stable to finite-amplitude perturbations than the cycle  $C_s$ . This difference in stability cannot be predicted by local analysis by means of multipliers and contradicts an initial expectation that the middle location of the saddle cycle between two stable cycles should correspond to a similar stability of the cycles. Thus, the Pontryagin approach provides an important means for characterization and comparison of the global stability of the cycles by calculating  $J_m^p$ . This analysis together with optimal energy minimization are the most significant results of the study.

The global stability, as shown in Fig. 4, depends on the working frequency  $\Omega$  in the hysteresis region. For cycle  $C_l$ , the barrier is relatively small and decreases to the point of saddle-node bifurcation (insert in Fig. 4). In contrast, the barrier  $J_m^p$  for  $C_s$  increases rapidly with  $\Omega$ . The behaviour of  $J_m^p$  is defined by the type of nonlinearity in (1). The barriers are equal for the cycles  $C_l$  and  $C_s$  in the vicinity of  $\Omega = 1.34$ . For this value of frequency the location of the saddle cycle is close to the stable cycle  $C_l$

(see the lower inset in Fig. 1). Similar barriers represent the same stability as well as similar energy of the control functions, whilst the shapes of the control functions are different.

In summary, we have discussed the minimal energy control for different control functions acting in a bistable nonlinear memory element. For pulse-type control functions  $u_1(t)$  and  $u_2(t)$ , we have identified a particular set of parameters culminating in a minimal control energy  $J_m$  and further analyzed the dependence of energy  $J$  on parameters of these functions. A drawback of the single pulse control  $u_1(t)$  consists in its strong dependence on the phase  $\phi_0$ , and is energetically less efficient than the function  $u_2(t)$ . Significantly, the Pontryagin approach in this study has led to the control function being characterized by a longer duration than  $u_1(t)$  and  $u_2(t)$ , but with a marked reduction of energy. With regard to the power consumption, the superiority of the Pontryagin control approach is clearly demonstrated. Furthermore, the value of minimal control energy  $J_m^p$  determined by Pontryagin approach is applied for the characterization of global stability of the oscillatory states and clearly demonstrates how these values  $J_m^p$  can be utilised in order to specify equally stable oscillatory states. The approach presented in this paper can be applied for other systems, for example the ferromagnetic layer<sup>16</sup> mentioned above.

- <sup>1</sup>I. Mahboob and H. Yamaguchi, Nat. Nanotechnol. **3**, 275 (2008).
- <sup>2</sup>B. Charlot, W. Sun, K. Yamashita, H. Fujita, and H. Toshiyoshi, J. Micromech. Microeng. **18**, 045005 (2008).
- <sup>3</sup>Y. Tsuchiya, K. Takai, N. Momo, T. Nagami, H. Mizuta, S. Oda, S. Yamaguchi, and T. Shimada, J. Appl. Phys. **100**, 094306 (2006).
- <sup>4</sup>Q. P. Unterreithmeier, T. Faust, and J. P. Kotthaus, Phys. Rev. B **81**, 241405 (2010).
- <sup>5</sup>W. J. Venstra, H. J. R. Westra, and H. S. J. van der Zant, App. Phys. Lett. **97**, 193107 (2010).
- <sup>6</sup>H. Noh, S.-B. Shim, M. Jung, Z. G. Khim, and J. Kim, App. Phys. Lett. **97**, 033116 (2010).
- <sup>7</sup>R. L. Badzey, G. Zolfagharkhani, A. Gaidarzhy, and P. Mohanty, App. Phys. Lett. **85**, 3587 (2004).
- <sup>8</sup>D. N. Guerra, M. Imboden, and P. Mohanty, App. Phys. Lett. **93**, 033515 (2008).
- <sup>9</sup>M. M. Mano and C. R. Kime, *Logic and computer design fundamentals*, 4th ed. (Pearson, Upper Saddle River; Harlow, 2008).
- <sup>10</sup>I. Kozinsky, H. W. C. Postma, O. Kogan, A. Husain, and M. L. Roukes, Phys. Rev. Lett. **99**, 207201 (2007).
- <sup>11</sup>J. F. Rhoads, S. W. Shaw, and K. L. Turner, J. Dyn. Syst.-T. ASME **132**, 034001 (2010).
- <sup>12</sup>P. Whittle, *Optimal Control Basics and Beyond* (John Wiley, Chichester, 1996).
- <sup>13</sup>D. G. Luchinsky, I. A. Khovanov, S. Beri, R. Mannella, and P. V. McClintock, Int. J. Bif. Chaos **12**, 583 (2002).
- <sup>14</sup>R. Graham and T. Tél, Phys. Rev. Lett. **52**, 9 (1984).
- <sup>15</sup>I. A. Khovanov, D. G. Luchinsky, R. Mannella, and P. V. E. McClintock, Phys. Rev. Lett. **85**, 2100 (2000).
- <sup>16</sup>Dunn T. and A. Kamenev, Appl. Phys. Lett. **98**, 143109(3) (2011).
- <sup>17</sup>I. A. Khovanov, N. A. Khovanova, E. V. Grigorieva, D. G. Luchinsky, and P. V. E. McClintock, Phys. Rev. Lett. **96**, 083903 (2006).
- <sup>18</sup>S. Beri, R. Mannella, D. G. Luchinsky, A. N. Silchenko, and P. V. E. McClintock, Phys. Rev. E **72**, 036131 (2005).
- <sup>19</sup>I. A. Khovanov, N. A. Khovanova, and P. V. E. McClintock, Phys. Rev. E **67**, 051102 (2003).